NANOSYSTEMS:
PHYSICS, CHEMISTRY, MATHEMATICS

Original article

AlHussein H., et al. *Nanosystems: Phys. Chem. Math.*, 2023, **14** (6), 633–643.
http://nanojournal.ifmo.ru
DOI 10.17586/2220-8054-2023-14-6-633-643

Study of the electrical and electronic properties of crystalline molybdenum disulfide (MoS_2-3R) semiconductor nano using alternating current (AC) measurements

Hussein Alhussein, Jamal Qasim AlSharr, Sawsan Othman, Hassan AlKhamisy

University of Aleppo, Syria

Corresponding author: Hussein Alhussein, husianphy990@gmail.com

ABSTRACT MoS_2 nanostructures were prepared using the hydrothermal method by reacting ammonium heptamolybdate tetrahydrate ($(NH_4)_6Mo_7O_{24}4H_2O$) with citric acid monohydrate ($C_6H_8O_7H_2O$) in distilled water with the presence of sodium sulfide (Na_2S). The surface structure studies of MoS_2 showed that the size of the surface clusters of the studied tablet is of the order of 50 – 100 nm. Using measurements (Zetasizer Nano Series), we found that the particle sizes ranged from 150 – 350 nm. Alternating current (LCR) measurements were made for (tablet-MoS_2) under a constant temperature $T = 10$ °C. Measurements of the parallel electrical capacitance (C_p) in terms of frequency (F) of tablet-MoS_2 showed a sharp drop in the value of the electrical capacitance (C_p) with an increase in frequency within the range 20 Hz – 16 kHz. It is shown that the series capacitance increased with the increase of the applied potential.

KEYWORDS MoS_2-3R, atomic force microscopy (AFM), LCR measurements, electrical capacitance, Zetasizer Nano Series

FOR CITATION AlHussein H., AlSharr J., Othman S., AlKhamisy H. Study of the electrical and electronic properties of crystalline molybdenum disulfide (MoS_2-3R) semiconductor nano using alternating current (AC) measurements. *Nanosystems: Phys. Chem. Math.*, 2023, **14** (6), 633–643.

1. Introduction

When studying semi-conducting materials of silicon or its compounds in nanoscale dimensions, scientists found that they are subject to quantum constraint. Therefore, these materials seem as if they have reached their practical limits and cannot be used in modern technologies and devices that depend on nanotechnology. Therefore, scientists began searching for new materials that have properties that meet the requirements of technological progress and molybdenum disulfide was among these materials, which is characterized by multiple structural phases that give it unique properties that enable it to be used in electronic, photovoltaic, or magnetic applications. MoS_2 is considered as one of the types of semiconductors that belong to the family of transition metal chalcogenides (TMDs) that consist of layers linked by van der Waals forces that allow the formation of several crystalline phases of dichalcogen MX2, where M belongs to the metallic elements in the periodic table within the groups It represents the element chalcogen [1,2]. MoS_2 is considered as one of the important and promising compounds of this group as a result of its important physical properties, where molybdenum disulfide (MoS_2-3R) is considered as a promising alternative to silicon because of its excellent photovoltaic properties and its gap with an energy equal to the energy gap 1.2 eV of silicon [3, 4], it also has a unique multilayer or single-layer structure. These properties make it an ideal material for future applications in semiconductors, transistors, chips, and other fields of advanced science and technology. Therefore, in recent years, scientists have maintained great interest in the exploration and research of molybdenum disulfide (MoS_2-3R) [5–7].

Molybdenum disulfide exists in three patterns 3R–2H–1T, the two patterns (2H, 1T) have a semi-metallic behavior, while the pattern 3R has a semi-conducting behavior, where the pattern MoS_2-3R is characterized by an energy gap similar to the energy gap of silicon in its structural state (bulck), the sulfide is distinguished by its multi-layered structure, where we will focus in this research on studying the electrical properties of molybdenum disulfide MoS_2-3R [8–10].

2. The importance of research:

In the present work, a characterization of the electrical properties of molybdenum disulfide MoS_2 prepared chemically in the form of nanostructures with a structure of the type MoS_2-3R using alternating current measurements. We also study the nodal resistance changes with the change of temperature of the studied sample in order to employ this compound in electronic applications The molybdenum sulfide in the type MoS_2-3R has a wide optical absorption in the infrared and visible light fields. In its structural state (bulk), it has an energy gap similar to the silicon gap. Therefore, a comprehensive electrical characterization of this compound must be made.

3. Practical and experimental study

3.1. The devices and tools used: instruments & devices

(1) Zetasizer Nano-Particle size and zeta potential measurement.
(2) Atomic Force Microscopy (AFM).
(3) X-ray spectroscopy (XRD) from Phywe.
(4) LCR meter (LCR meter-microtest-6379).
(5) Chemical preparation tools (accurate electronic balance, desiccant, and thickened).
(6) Magnetic mixer with heater model (502p-2) from the American company PMC.

3.2. Materials used, method and stages of preparation

3.2.1. Materials used. Ammonium heptamolybdate tetrahydrate ($(NH_4)_6Mo_7O_{24}$ $4H_2O$), tetrathiomolybdate ammonium, distilled water, citric acid monohydrate ($C_6H_8O_7$ H_2O).

3.2.2. Method of preparation. To prepare nanostructures from 3R-MoS_2, the preparation process was carried out using the hydrothermal method [11], where in the manufacturing process, sodium sulfide was used as a source of sulfur in order to obtain molybdenum sulfide through chemical reactions, and thus we have obtained a pure powder of Molybdenum sulfide as shown in Fig. 1. Where we pressed an amount of this powder amounting to $M = 1$ gr, we obtained a MoS_2-Tablet with a diameter of 15 mm and a thickness of 2 mm for the electrical characterization, using a hydraulic compressor with a capacity of 5 ton/cm^2, and without heat treatment (the tablets have not been heat treated).

(a) (b)

FIG. 1. Pure powder prepared from MoS_2 (a); MoS_2 powder prepared and compressed into tablets (b)

3.3. Measurements (Zetasizer Nano Series) of formed nanoparticles

To determine the size of the formed nanoparticles, we measured the size of these granules using the Zetasizer Nano device, model ZS-Nano, produced by Malvern Company, using a red laser source, with a wavelength of 632.8 nm. We placed a suspension of molybdenum sulfide (MoS_2) in quartz cells designated for the device. The device is calibrated at a constant temperature of 25 °C. The dimension of the scanned cell are 5.5 mm, and a count rate is 141.8 = count rate (k_{cps}), so we found that the particle sizes ranged from 150 – 350 nm and that the average particle size was equal to 267 nm as shown in Fig. 2.

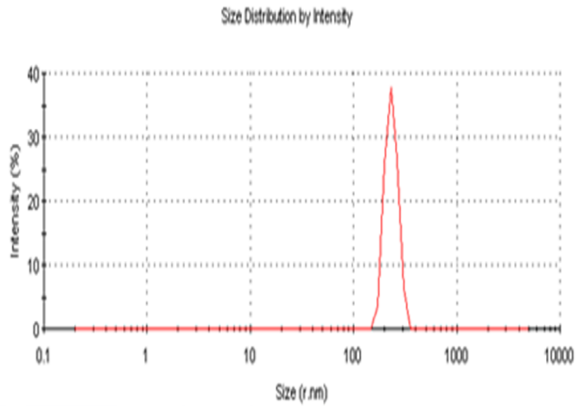

FIG. 2. Zetasizer Nano Series measurements of the size of the prepared MoS_2 granules

3.4. X-ray diffraction spectrum

In order to verify the structure of the prepared molybdenum disulfide, the crystallization of the prepared samples was studied by using an X-ray device produced by Phywe company and applying a current which intensity is 0.1 mA and an angle hop of 0.1 degrees every 10 sec). Measurements between angles 80° – 10° were taken and a copper anode which wavelength 1.541 Å was used.

X-ray spectra (XRD) of the nanopowder prepared from MoS_2 showed that there are no clear peaks, and this indicates and confirms the nanostructure of MoS_2 is amorphous, and this is consistent with the data of the card (JCPDS No. 06-0097) [12–14], as in Fig. 3(a). Since the crystallization process in the patterns (1T, 2H) is related to pressure and the degree of oxidation, we prepared tablets with diameters of 1.5 cm and thickness of 3 mm from powder-MoS_2 using a hydraulic compresser by subjecting powder-MoS_2 to a pressure of 5 ton. The X-ray diffraction measurements of these discs showed the presence of a very clear and intense peak corresponding to the crystalline plane (002) corresponding to the degree ($2\theta = 14.6°$). This is consistent with the values of the aforementioned molybdenum disulfide reference cards. Fig. 3(b) shows the presence of several diffraction peaks. It means that there are several phases within the structure of MoS_2.

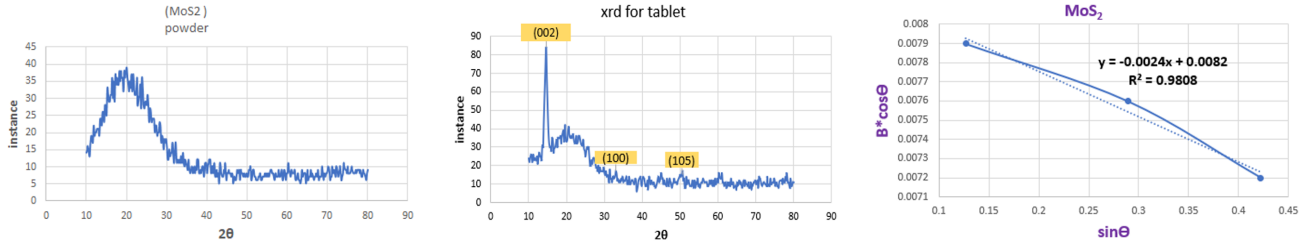

(a) (b) (c)

FIG. 3. XRD of nanopowder prepared from MoS_2 (a); XRD of nanopowder prepared from MoS_2 (b); Representing the W–H relation (c)

Table 1 shows the diffraction angles and corresponding crystal planes.

TABLE 1. The diffraction angles and corresponding crystal planes

2θ	14.6	32.5	50
(hkl)	(002)	(100)	(105)

The (002) crystal plane is the preferred crystal plane for MoS_2 crystals, as shown in Fig. 3(b). In accordance with Bragg's law of the X-rays diffraction (1), the distance between the crystal planes defined by Miller's indices (hkl) can be set:

$$2d_{hkl}\sin(\theta_{hkl}) = n\lambda. \tag{1}$$

Here d_{hkl} represents the distance between the parallel crystal planes according to the hkl direction, the angle θ_{hkl} is the diffraction angle, and n is the diffraction rank, λ represents the wavelength of the X-rays ($\lambda = 1.541$ Å). By calculation, it turns out that the value of the lattice constant is $d_{hkl} = 5.906$ Å, and by using the Williamson–Hall relation, which is given by relation (2):

$$\frac{1}{D} + \frac{2\varepsilon\sin\theta}{\lambda} = \frac{\beta\cos\theta}{\lambda}. \tag{2}$$

Other parameters can be determined from the X-ray spectra, such as the size of crystallization and strain of the crystal lattice, where β is the width of the mid-intensity of each peak estimated in radians, D is the size of crystallization, ε is the effective tension between atoms within the structure, and λ is the wavelength of the X-rays used. By plotting the previous relation, where it represents the point of interpart (λ/D) and the slope represents 2ϵ and the W–H relation can be represented in Fig. 3(c).

By calculation, we found that:

$$\frac{\lambda}{D} = 0.0082 \quad \Rightarrow \quad D = \frac{\lambda}{0.0082} = \frac{1.5418}{0.0082} = 192.7\ \mathring{A} = 19.27\ \text{nm}.$$

The value of the lattice constants (a) is calculated from relation (3):

$$d_{hkl} = \frac{a}{\sqrt{h^2 + k^2 + l^2}}. \tag{3}$$

By calculation $d_{hkl} = 5.906$ Å, the atomic dislocations within the crystal structure can be calculated based on the XRD spectrum using relation (4) [15, 16]:

$$\delta = \frac{14\beta \cos\theta}{4aD} = 0.0152 \ \left(\text{Lin nm}^{-1}\right), \tag{4}$$

where higher values of δ indicate lower crystallinity levels of the films and amount of defects in the structure.

3.5. Studying the surface structure of molybdenum disulfide MoS_2-Tablet using AFM atomic force microscopy

Using atomic force microscopy AFM, a microscopic picture of the surface of the tablets prepared from molybdenum sulfide powder (MoS_2-Tablet) was taken, where we used different sizes and the same area of the sample surface (3 μm × 3 μm) (1.01 μm × 1.01 μm).

These images showed the shape of the surface atomic clusters on the surface, where the average size of the atomic clusters formed in the structure of the surface of the MoS_2-Tablet was determined, as the formed sizes ranged between 50 – 150 nm as shown in Fig. 4, where the crystalline phases of MoS_2 are formed under the process of hydraulic pressure.

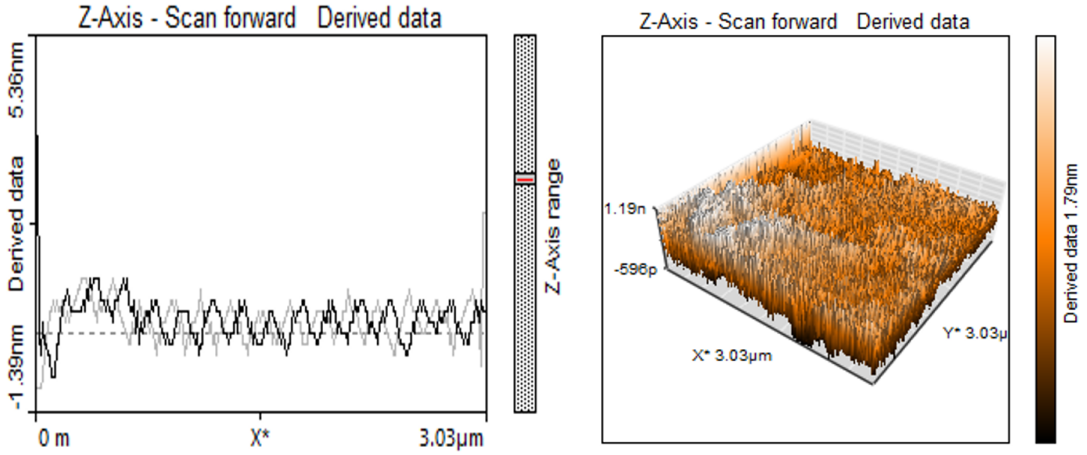

(a) (b)

FIG. 4. AFM images of tablet molybdenum disulfide at two scales (3 μm × 3 μm), (1.01 μm × 1.01 μm)

3.6. Measurements of alternating current (AC)

Alternating current measurements (capacitance, conductivity, electrical resistance, and parallel resistance (R_p values of the nanostructures were studied using a LRC meter within a frequency range 20 Hz – 1 MHz and applying an alternating potential 3 V at a room temperature $T = 11$ °C.

3.6.1. Electrical parallel capacitance C_p. Parallel capacitance (C_p) measurements as a function of frequency (F) under constant temperature ($T = 11$ °C) showed a sharp decrease in the C_p value with increasing frequency within the range 20 Hz – 16 kHz, after which it decreases. Parallel capacitance gradually as shown in Fig. 5, where the capacitance is $C_p = 4500$ pF at frequency $F = 20$ Hz, and decreases dramatically. Very close to the value $C_p = 44.8$ pF is obtained at the frequency 16 kHz, where the capacitance changes become constant with increasing frequency from 1000 –16 kHz.

But in the frequency range 16 – 300 kHz, the changes in the parallel electrical capacitance C_p become gradual, ranging from $C_p = 44.8$ – 17 pF The changes in the parallel electrical capacitance C_p become slight and almost constant in the frequency range 300 – 1000 kHz, where the changes in the capacitance corresponding to this frequency range is as follows: $C_p = 14$ – 17 pF, as shown in Fig. 6.

This change in the electrical capacitance of the molybdenum sulfide discs in terms of frequency is explained by the return to the polarization mechanisms that occur at different frequencies. At frequency less than 300 KHz, the four polarization mechanisms (electronic, ionic, orientational spacecharge) occur. This polarization includes displacement of charges either by orientation (i.e. directional polarization) or by migration of charge carriers (such as hopping polarization or space charge). The parallel capacitance relation with the loss factor is given by the relation (5) [17, 18]:

$$D = \frac{1}{W \cdot R_P \cdot C_p}. \tag{5}$$

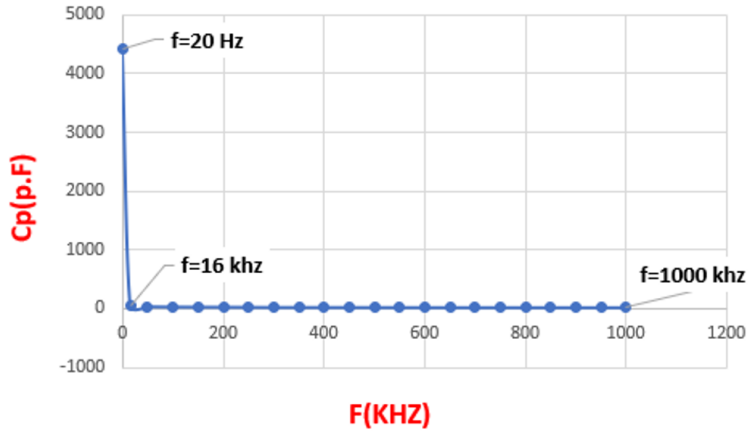

FIG. 5. Variations of the parallel electrical capacitance (C_p) with frequency (F)

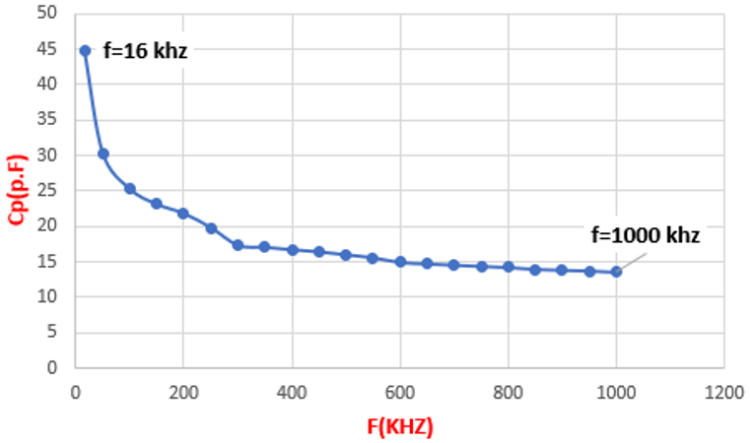

FIG. 6. Variations of the parallel electrical capacitance (C_p) with frequency (F) between 16 – 300 kHz

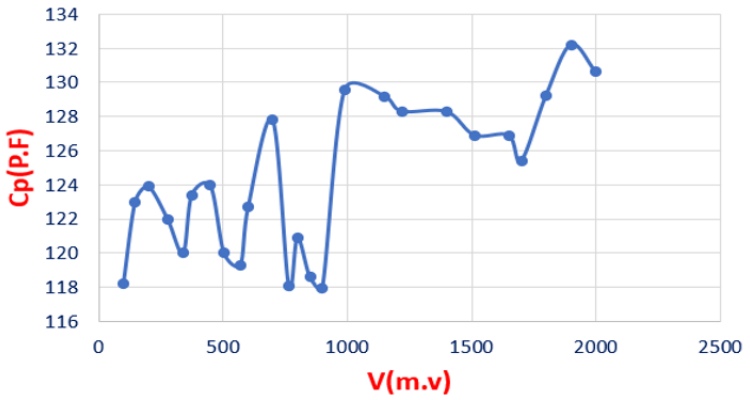

FIG. 7. Variations of the parallel electrical capacitance C_p, with the electric potential V

3.6.2. Parallel capacitance changes C_p with potential V. When studying the changes of the parallel capacitance C_p with the change in the potential applied to MoS_2-Tablet, it was shown that the electrical capacitance values of crystalline molybdenum change with the change of electrical potential as shown in Fig. 7.

For applied potentials 145 – 900 mV, it is similar to an alternating current wave, while for higher potentials in a range of 1000 – 2000 mV, the electrical capacitance changes are semi-regular and ranges between 132 –125 pF.

3.6.3. Determining the type of semiconductor. To determine the type of semiconductor, the electrical capacitance changes were studied with the electric potential within the range of 0.05 – 1.8 V, and at a frequency of $F = 1$ KHz and at a room temperature $T = 9$ °C. By plotting the changes of $\left(\frac{1}{C} - \frac{1}{2C_0}\right)^2$ in terms of V (Volt) according to the relation (8):

$$\left(\frac{1}{C} - \frac{1}{2C_0}\right)^2 = \frac{2}{\varepsilon e\,(N_d - N_a)}(\Psi + V). \tag{6}$$

From Fig. 8, we notice that the slope of the graph line representing the changes is negative and therefore $N_a \gg N_d$, and this means that the semiconductor is of type p.

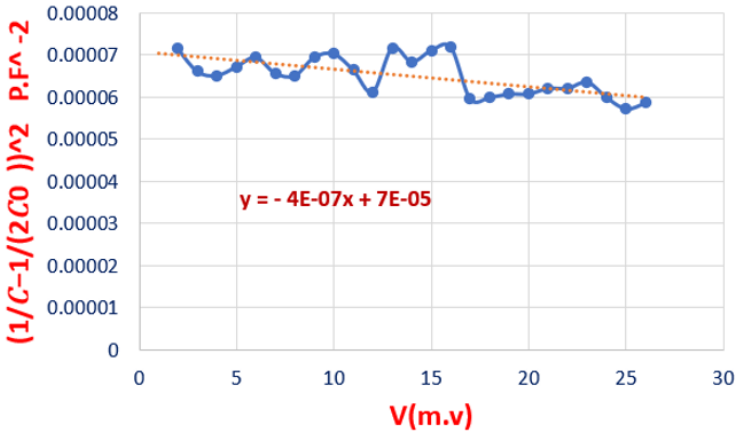

FIG. 8. $\left(\frac{1}{C} - \frac{1}{2C_0}\right)^2$ changes with potential

3.6.4. Parallel Electrical Resistance (RP) of MoS_2-Tablet. Measurements of the parallel resistance RP of crystallized molybdenum disulfide MoS_2-Tablet show semi-regular behavior which is completely different from the behavior of morpho molybdenum sulfide, where it was found that the electrical resistance RP decreases in the range 1500 – 108 KΩ in the low frequency diapason 20 Hz – 100 KHz. Then the resistance increases again at the frequency 200 KHz and the resistance value becomes 130 KΩ and then it returns to decreasing as shown in Fig. 9, the RP resistance changes become constant and range from 30 – 70 KΩ in the frequency range 1000 KHz – 250 KHz.

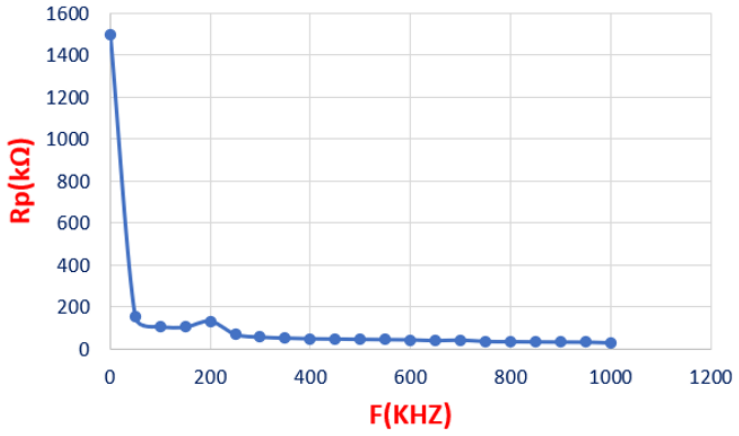

FIG. 9. Parallel resistance (R_P) changes with frequency intensity (F)

We note from the previous figure, that the resistance changes are a sharp decrease in the parallel resistance values RP at low frequencies and the parallel resistance changes become simple at high frequencies, and the parallel resistance is related to both the quality factor and the parallel inductance by the relation (7) [19]:

$$R_P = R_S\left(1 + Q^2\right) = QwL_P. \tag{7}$$

3.6.5. Capacitive Electrical Resistance (Xc) of MoS_2-Tablet. The measurements showed that the absolute value of the capacitive resistance of crystallized molybdenum disulfide (X_c) decreases sharply with the frequency at low frequencies, then the changes become small and gradual as shown in Fig. 10, where it is found that the changes of X_c are sharp with the frequency within a range of frequencies 20 Hz – 200 KHz, and in the range of frequencies 50 Hz – 3000 KHz the value of X_c changes gradually with increasing frequency.

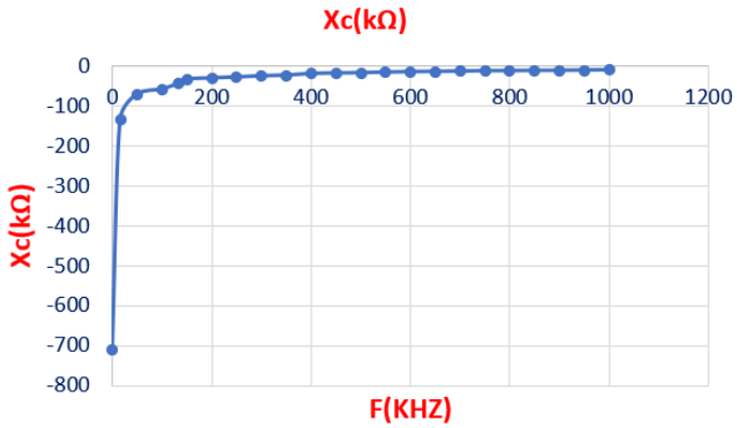

FIG. 10. Changes of capacitive resistance X_c in crystallized molybdenum disulfide with frequency F

As the frequency applied to MoS_2-Tablet increases, it leads to reducing of the capacitive resistance. Likewise, when the frequency applied to MoS_2-Tablet decreases, its capacitive resistance value increases. As the frequency increases, the MoS_2-Tablet passes more charge, which leads to a larger current flow between the electrodes, which appears as if the internal impedance (capacitive resistance) has decreased, so the value of the capacitive resistance is "frequency dependent". Whereas, the value of capacitive resistance is given by the relation:

$$X_c = \frac{-i}{\omega C},$$

where X_c is the capacitive resistance, ω is the angular frequency ($\omega = 2\pi F$), and C is the capacitance of the capacitor. Several facts are evident from this formula alone. The X_c is of an ideal capacitor, and therefore its impedance, is negative for all values of capacitance.

3.6.6. Series Electrical Capacitance (C_s). Series electrical capacitance C_s changes with frequency F. Measurements of the series electrical capacitance C_s in terms of frequency F showed a sharp drop in the value of electrical capacitance $C_p = 70$ – 980 pF (see Fig. 11) with an increase in frequency within the range 20 Hz – 16 kHz.

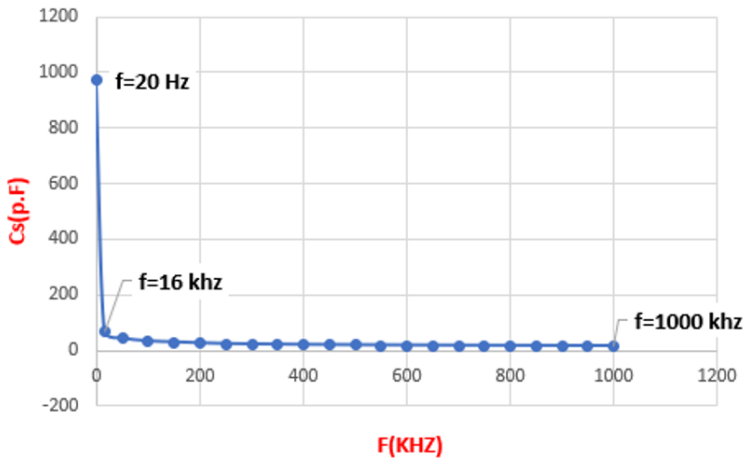

FIG. 11. Variations of series electrical capacitance C_s with frequency F

The series capacitance C_s decreases gradually with the frequency increase from 16 – 300 kHz, under a constant temperature $T = 10$ °C, as shown in Fig. 12.

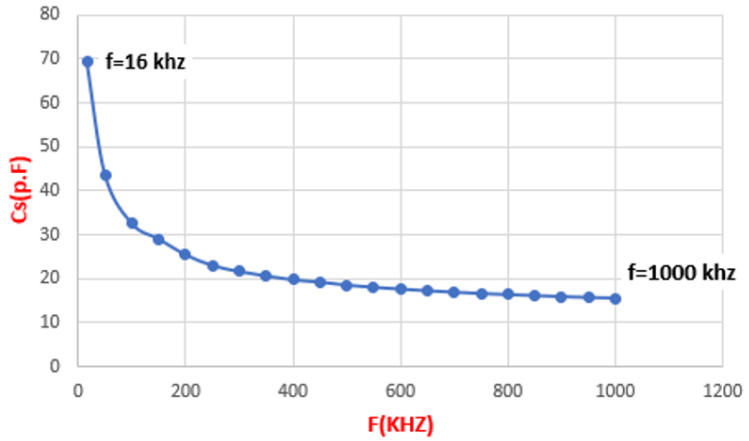

FIG. 12. Variations of series electrical capacitance C_s with frequency F between 16 – 1000 kHz

The series electrical capacitance changes C_s become slight and almost constant at the frequency range 300 – 1000 kHz, where the corresponding capacitance changes for this frequency range are $C_s = 20$ – 15 pF as shown in the Fig. 12.

3.6.7. Series electrical capacitance variations C_s with potential V. When studying the changes of the series capacitance C_s with the change of the applied potential on MoS_2-Tablet, it was found that the changes of the series electrical capacitance range from increasing and decreasing within the range of low potential 50 – 350 mV as shown in Fig. 13. The series capacitance increased gradually and slightly with the increase of the applied potential in the range 250 – 900 mV, C_s having a sharp dip for the potential 950 mV as shown in Fig. 13.

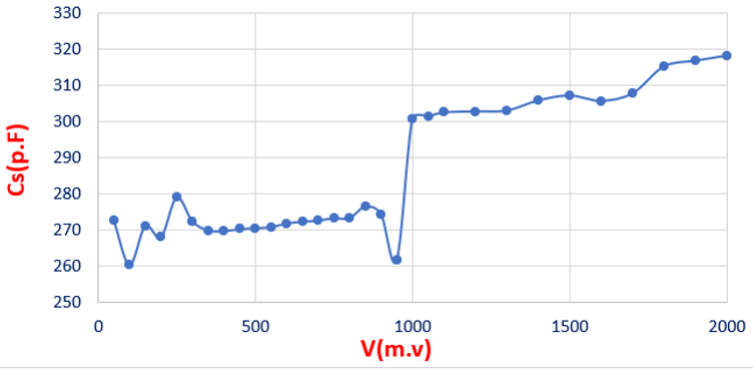

FIG. 13. Variations of the parallel electrical capacitance C_p with the electrical potential V

The series capacitance changes becomes increasing 300 – 320 pF with applied potential 1000 – 2000 mV as shown in Fig. 13.

3.6.8. Parallel induction study (L_p) of crystalline molybdenum sulfide MoS_2-Tablet. From studying the changes of the parallel inductance L_p with the frequency F, it was found that the absolute value of L_p decreases very sharply from the value 48390 mH to the value 2 mH at low frequency $F = 0.02$ – 50 KHz as shown in Fig. 14.

For values of frequency of 50 – 1000 KHz, the parallel inductance changes become decreases and slight as shown in Fig. 15, until the absolute value of the parallel inductance ranging between $L_p = 0.1$ – 0.02 mH at the frequency 1000 KHz. However, there is a response and a jump in the parallel inductance at frequency 350 KHz, where value of the parallel inductance becomes $L_p = 0.267$ mH as shown in Fig. 15. Parallel inductiveness is related to the quality factor by the relation (8) [20]:

$$Q = \frac{1}{D} = \frac{wL_S}{R_S} = \frac{R_P}{wL_P}. \tag{8}$$

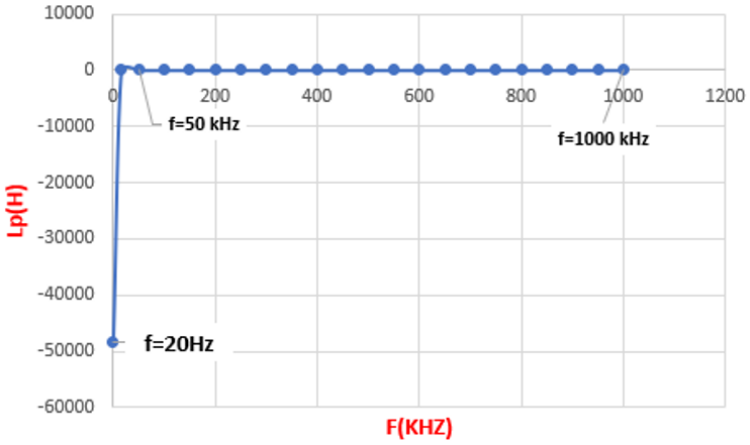

FIG. 14. Variations of parallel inductance L_p with frequency F

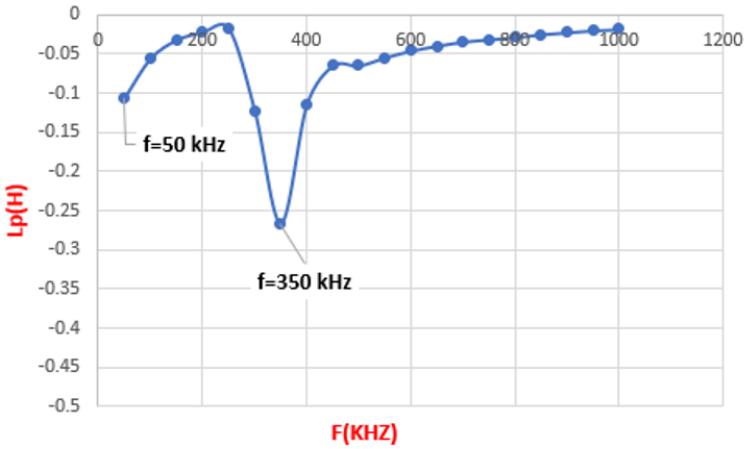

FIG. 15. Variations of Parallel Inductance L_p with Frequency F between 50 – 1000 kHz

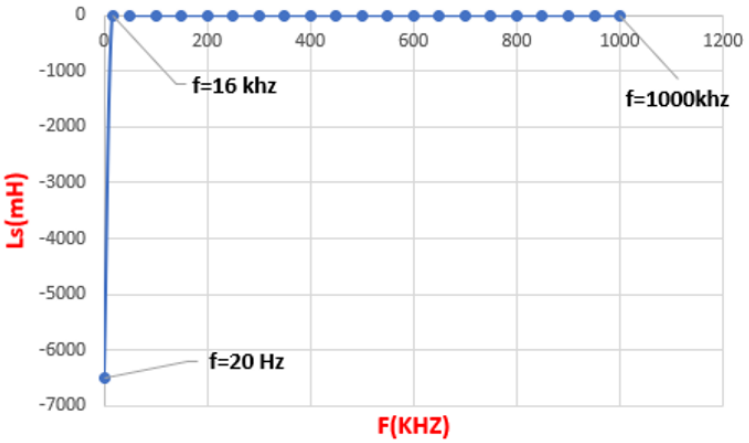

FIG. 16. Variations of series inductance L_s with frequency F

3.6.9. Series induction study Ls of crystalline molybdenum disulfide (MoS_2-Tablet). From studying the parallel inductance changes of L_s with frequency F, it was found that the absolute value of L_s decreases very sharply from the value of 6500 mH to the value of 1.3 mH at low frequency $F = 0.02 - 16$ KHz as shown in Fig. 16.

For frequencies in the range $F = 100 - 1000$ KHz we find that the changes in series inductance become slight and gradual as the absolute value of the inductivity of L_s is between 0.07 – 0.01 mH. We notice the appearance of a peak and increase in series inductance at frequency $F = 650$ KHz to value 0.367 as shown in Fig. 17.

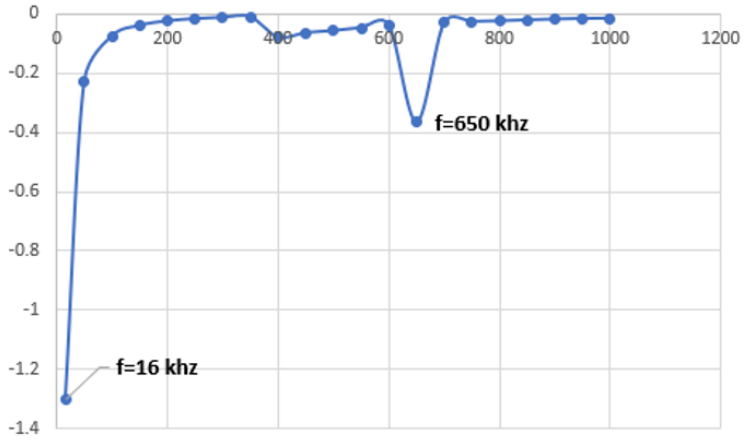

FIG. 17. Variations of series inductance L_s with frequency F between 16 – 1000 KHz

4. Conclusion

(1) The XRD spectrum of the powder prepared from MoS_2 showed that its structure is morphic and amorphous, and with a process using a hydraulic press, the structure becomes crystalline. We observe the appearance of a preferred crystallization level 200 at $2\theta = 14.6^\circ$.

(2) The AFM images show that the surface atomic clusters of the surface of the molybdenum sulfide sample (MoS_2-Tablet) range between 50 – 150 nm, where it is clear that the crystalline phases of MoS_2 are formed under the process of hydraulic pressure.

(3) Measurements of the parallel electrical capacitance (C_p) in terms of frequency (F) of (tablet-MoS_2) showed a sharp drop in the value of the electrical capacitance C_p with an increase in frequency within the range 20 Hz – 16 kHz.

(4) Measurements of the series electrical capacitance (C_s) in terms of frequency (F) showed a sharp drop in the value of electrical capacitance $C_p = 980 - 70$ pF, after which the series capacitance C_s decreases gradually, where the capacitance changes become constant with the frequency increase from 200 – 1000 KHz.

References

[1] Kuc B., Heine T. On the Stability and Electronic Structure of Transition Metal Dichalcogenide Monolayer Alloys Mo1-x Xx-S2-y Sey with X = W, Nb. *Electronics*, 2016, **5**, P. 1201–1213.

[2] Voiry D., Mohite A., Chhowalla M. Phase engineering of transition metal dichalcogenides. *Chem. Soc. Rev.*, 2015, **44**, 2702.

[3] Mak K.F., Lee C., Hone J., Shan J., Heinz T.F. Atomically thin MoS_2: anew direct-gap semiconductor. *Phys. Rev. Lett.*, 2010, **105**, 136805.

[4] Radisavljevic, Radenovic A., Brivio J., Giacometti V., Kis A. Preparation and Application of Graphene-like Tungsten Sulfide Thin Films by Chemical Vapor Deposition. *Nat Nano*, 2011, **6**, P. 147–152.

[5] Hernandez Ruiz K., Liu J., Tu R., Li M., Zhang S., Vargas Garcia J.R., Mu S., Li H., Goto T., Zhang L. Effect of microstructure on HER catalytic properties of MoS_2 vertically standing nanosheets. *J. Alloys Compd*, 2018, **747**, 100.

[6] Deng Z.H., Li L., Ding W., Xiong K., Wei Z.D. Synthesized ultrathin MoS_2 nanosheets perpendicular to graphene for catalysis of hydrogen evolution reaction. *Chem. Commun.*, 2015, **51**, 1893.

[7] Wang Y., Yu L., Lou X.W. Synthesis of highly uniform molybdenum–glycerate spheres and their conversion into hierarchical MoS_2 hollow nano spheres for lithium-ion batteries. *Angew. Chem. Int. Ed.*, 2016, **55**, 7423.

[8] Mervin Zhao, Ziliang Ye, Ryuji Suzuki, Yu Ye, Hanyu Zhu, Jun Xiao, Yuan Wang, Yoshihiro Iwasa, Xiang Zhang. Atomically phase-matched second-harmonic generation in a 2D crystal. *Light: Science & Applications*, 2016, **5**, e16131.

[9] Guo C., et al. Observation of superconductivity in 1T'-MoS_2 nanosheets. *J. of Materials Chemistry C*, 2017, **5**, 10855.

[10] Fang Y., et al. Structural determination and nonlinear optical properties of MoS_2 compound. *JACS*, 2019, **141**, 790.

[11] Al-Hussein H., Al-Sharr J., Othman S., Khamisi H. Study of the electronic, (structural and optical) properties of MoS_2 nanostructures. *Aleppo University Research J.*, 2023, **170**, 1656.

[12] Mmantsae Diale, Nolwazi Nombona, Pannan I. Kyesmen, Lebogang Manamela. Electrically Enhanced Transition Metal Dichalcogenides as Charge Transport Layers in Metallophthalocyanine-Based Solar Cells. *Frontiers in Chemistry*, 2020, **8**.

[13] Sathiyan S., Ahmad H., Chong W.Y., Lee S.H., Sivabalan S. Evolution of the Polarizing Effect of MoS_2. *IEEE Photonics J.*, 2015, **7** (6), 6100610.

[14] Callegro L. *Electrical Impedance: Principles, Measurement, and Applications*. New York: CRC Press, 2013.

[15] Sathe D.J., Chate P.A., Subrao Subrao Sargar, Kite S.V. Properties of chemically-deposited nanocrystalline MoS_2 thin films. *J. of Materials Science: Materials in Electronics*, 2016, **27** (4).
[16] Singh J., Verma N.K. Structural, optical and magnetic properties of cobalt-doped CdSe(MPA) nanoparticles. *Bull. Mater. Sci.*, 2014, **37** (3), P. 541–547.
[17] Oliver B.M., Cage J.M. *Electronic Measurement and Instrumentation*, McGraw-Hill, New York, 1971.
[18] Grover F. *Inductance Calculations (Dover Books on Electrical Engineering)*, Dover Publications, 2009.
[19] Jun He, Laizhou Song, Jiayun Yan, Ning Kang, Yingli Zhang, Wei Wang. Hydrogen Evolution Reaction Property in Alkaline Solution of Molybdenum Disulfide. *Metals*, 2017, **7** (6), 211.
[20] Pawelec B., Navarro R., Fierro J.L.G., Vasudevan P.T. Studies of molybdenum sulfide catalyst ex ammonium tetrathiomolybdate: effect of pretreatment on hydrodesulfurization of dibenzothiophene. *Applied Catalysis A: General*, 1998, **168**, P. 205–217.

Submitted 17 September 2023; revised 26 September 2023; accepted 21 November 2023

Information about the authors:

Hussein Alhussein – Department of Physics, faculty of Science, University of Aleppo, Syria; ORCID 0009-0007-4525-9664; husianphy990@gmail.com

Jamal Qasim AlSharr – Department of Physics, faculty of Science, University of Aleppo, Syria;

Sawsan Othman – Department of Physics, faculty of Science, University of Aleppo, Syria;

Hassan AlKhamisy – Institute of Health Technology, University of Aleppo, Syria; ORCID 0009-0006-5276-6560;

Conflict of interest: the authors declare no conflict of interest.